1.4 μm band emission properties of Tm^{3+} ions in transparent glass ceramics containing PbF$_2$ nanocrystals for S-band amplifier

Hideaki Hayashi
Graduate School of Human and Environmental Studies, Kyoto University, Kyoto 606-8501, Japan

Setsuhisa Tanabe[a]
Faculty of Integrated Studies, Kyoto University, Kyoto 606-8501, Japan

Teiichi Hanada
Graduate School of Human and Environmental Studies and Faculty of Integrated Studies, Kyoto University, Kyoto 606-8501, Japan

Tm^{3+} ion doped transparent oxyfluoride glass ceramics containing PbF$_2$ nanocrystals were prepared and infrared fluorescence properties of Tm^{3+} ions were investigated. From luminescence decay measurement, it is revealed that part of the Tm^{3+} ions were incorporated into fluoride crystals by annealing as-made glass above glass transition temperature. Temperature dependence of the 1.4 μm band emission properties of Tm^{3+} ions in transparent glass ceramics was investigated. With lowering temperature, the intensity ratio of the 1.4 μm emission band to the 1.8 μm band increased. At the same time, the center of gravity of the $^3H_4-^3F_4$ emission shifted to a longer wavelength and it reached about 1485 nm at 25 K. Under 50 K, the peak of the 1.4 μm band split and then the shape of the spectra became flatter. These properties can be utilized for the 1.5 μm (S-band) optical amplifier. © *2001 American Institute of Physics.* [DOI: 10.1063/1.1335645]

I. INTRODUCTION

As a result of an urgent demand for the increase of information capacity, considerable research efforts have been made to develop fiber amplifiers for wavelength division multiplexing (WDM) network systems. Since silica-based transmission fibers have a wide window from 1.4 to 1.7 μm, amplification of all these ranges is essential for a broad WDM network. Currently a gain band of 1530–1600 nm ($C+L$-band) is realized by development of an erbium-doped fiber amplifier.[1,2] The 1450–1480 nm band (S^+-band) has been also developed by a thulium-doped fiber amplifier (TDFA), although this band has some practical difficulties. Thus an upconversion pumping scheme[3] and a codoping manner have been proposed to improve the performance.[4,5]

To broaden the telecommunication range, it is required to explore an optical amplifier around 1500 nm (S band), the intermediate region of the $C+L$-band and S^+-band. Recently, this gain band has been realized by shifting the TDFA gain band to a longer wavelength region using a dual pumping scheme[6] or a high Tm^{3+} concentration doping technique.[7] In this article, we show another possibility of gain shifted TDFA by investigating fluorescence properties at lower temperatures.

Because in this band, the energy gap from the initiated $^3H_4$ level to the next lower level is relatively small, the materials with lower phonon energy are required as a luminescent host to suppress the nonradiative loss and to obtain higher quantum efficiency of the $^3H_4-^3F_4$ emission at 1.4 μm (refer to the energy diagram in Fig. 1). However, most
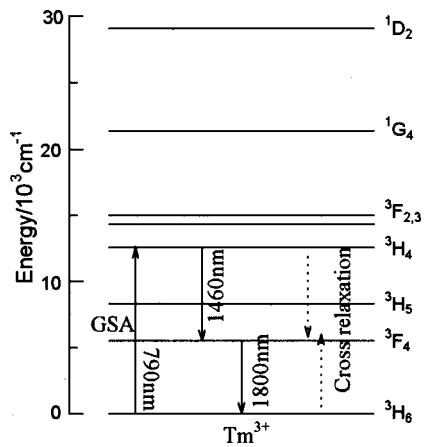
oxide glasses have large phonon energy (>1000 cm^{-1}) due to the stretching vibration of network-forming oxides. Fluoride glasses have the advantage due to their low phonon energy (300–500 cm^{-1}) and thus higher quantum efficiency of many active transitions.[8] However, the stability and fiberizability as a practical material still remain a problem. For the 1.4 μm fiber amplifier, fluoride-based TDF has been used but it has slightly poor chemical durability.

The invention of rare earth ion doped transparent oxyfluoride glass ceramics containing PbF$_2$ nanocrystals[9] has attracted much interest due to their excellent optical properties such as fluoride crystals and good mechanical, chemical properties such as oxide glasses.[10] In addition, for this material, Tick *et al.* have recently developed a low-loss fiber for an amplifier.[11] The advantages of these materials are that the rare earth ions can be incorporated into the fluoride crystal phase with lower phonon energy after heat treatments and the material remains transparent due to the much smaller size of precipitated crystals than the wavelength of visible light. In this study, the Tm^{3+}-doped glass ceramics containing PbF$_2$ were prepared and the possibility of this material being used for an optical amplifier is shown by investigating the lifetime of excited levels for various ceramming temperatures. Furthermore, for the possibility of gain shifted TDFA, the temperature dependence of fluorescence spectra was also investigated.
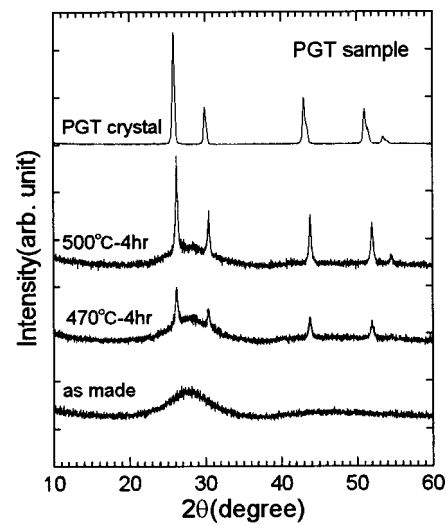
II. EXPERIMENT

The composition of the glass batch used for this study is shown in Table I. Expecting that the substitution of Tm^{3+} ion for the Pb^{2+} site in PbF$_2$ will become easier, fluoride components were mixed and sintered at 480 °C for 10 h with

---
[a]Author to whom correspondence should be addressed; electronic mail: tanabe@chem.h.kyoto-u.ac.jp

FIG. 1. Energy level diagram of Tm^{3+} ion and some transitions.

FIG. 2. XRD pattern of Tm^{3+}-doped glass ceramics (PGT sample) at various ceramming temperatures.

Ar atmosphere before melting the glass batch. After that, 0.1 mol (about 15 g) of the batch was melted in a platinum crucible at 1200 °C for 70 min in air atmosphere. The melt was cast into a stainless mold and we obtained a transparent glass sample for visible light. Then it was annealed for 1 h at 50 °C under glass transition temperature. T_g was obtained by using differential thermal analysis (Shimadzu, DTA-50) with 10 °C/min heating rate. The measured T_g of as-made glass was 447–457 °C. The annealed glass samples were cut into pieces $10 \times 10 \times 2$ mm^3 in size. After that, heat treatments from 450 to 510 °C for 4 h were performed to precipitate crystals. The sample pieces were polished for optical measurements. To confirm the precipitation of fluoride crystals, the x-ray diffraction (XRD) measurement (Shimadzu, XRD6000) was carried out with 2°/min scan speed from 10° to 60° 2 θ in 0.02 increments. Reference crystals correspond to the composition of fluoride components in the glasses (PGT or PYT crystal) were made and the XRD measurement also carried out to confirm the formation of a solid solution.

Infrared fluorescence spectra were measured with a monochromator (Nikon, G-250) controlled with a computer, and a PbS photodiode (HAMAMATSU, P4638) detector, and a lock-in amplifier (NF Electronic Instruments, LI-570A) were used. A diode laser of 792 nm (SONY, 304XT) was used as an excitation source and a silicon filter was installed in front of the monochromator to prevent laser scattering. Sensitivity calibration of the measurement system was done with a spectrum of a standard halogen lamp. For fluorescence spectra measurement at lower temperatures, a He cycling cryostat (Iwatani Plantec, TCU4) was used to

vary the temperature of glass ceramic samples from 15 to 300 K. For luminescence decay measurement of the $^3H_4$ level ($\lambda_{em} = 1460$ nm), the 792 nm diode laser was modulated into pulse with a function generator and an InGaAs photodiode (Electro-Optical System IGA-010-H, $f = 160$ kHz) was used as a detector. The signal of the photodiode was collected by a digital oscilloscope (LeCroy LS140, 100 MHz) and the lifetime was determined by least-square fitting of the decay curve with a single exponential function. The error of the lifetime data was less than ±20 μs.

III. RESULTS

A. X-ray diffraction and transparency

Variation of the XRD patterns of the PGT sample in the ceramming process is shown in Fig. 2. It can be seen that the as-made glass is completely amorphous with no diffraction peaks of crystals. With heat treatments, several broad peaks appeared, all of which were attributed to the PbF$_2$ crystal. At the same time, the width of the peaks became sharper with increasing ceramming temperature. The pattern of the PYT sample had almost the same characteristics as PGT. On the other hand, for the PT sample, no crystalline peaks appeared even after heat treatments. The glass ceramics kept transparency under 470 °C for the PGT and PYT samples, then became opaque at 500 °C.

TABLE I. Notation and composition for glass preparation.

	SiO$_2$	GeO$_2$	AlO$_{1.5}$	TiO$_2$	PbF$_2$	TmF$_3$	GdF$_3$	YF$_3$
PT	27.78	11.11	16.67	3.33	(41.07	0.04)^a		
PGT	25	10	15	3	(36.96	0.04	10)^b	
PYT	25	10	15	3	(36.96	0.04		10)^c

^{a}PbF$_2$–TmF$_3$ crystal used for glass preparation.
^{b}PbF$_2$–GdF$_3$–TmF$_3$ crystal used for glass preparation.
^{c}PbF$_2$–YF$_3$–TmF$_3$ crystal used for glass preparation.
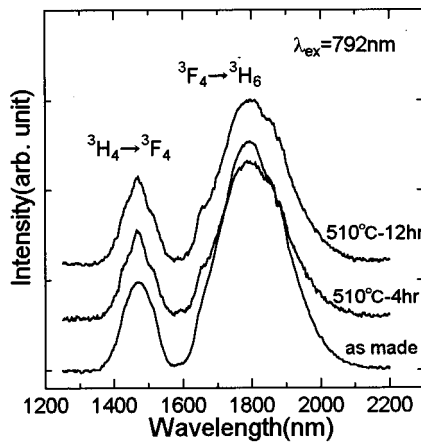
FIG. 3. Infrared fluorescence spectra of PGT sample heat treated for various times.

FIG. 5. Temperature variation of infrared fluorescence spectra in Tm^{3+}-doped transparent glass ceramics containing PbF_2 (PGT sample).

B. Fluorescence properties at room temperature

The room temperature fluorescence spectra of the PGT sample with various ceramming time (510 °C heat treatments) are shown in Fig. 3. The excitation wavelength was 792 nm. It can be seen that after cerammization, the emission bands showed sharper structure and inhomogeneous widths decreased. In this process, the relative intensity ratio of the 1460 nm emission to 1800 nm increased by 1.5 times with ceramming time. Similar tendency was observed for ceramming temperature. Figure 4 shows the $^3H_4$ lifetime with various ceramming temperatures obtained from the decay curves of the 1460 nm emission. The apparent lifetime of PGT and PYT crystal was 1.22 and 1.19 ms, respectively. For the PGT and PYT glass sample, it gradually increased by cerammization and finally became close to 500 μs. On the other hand, for the PT sample, it was almost unchanged. The lifetime of PGT and PYT glass samples also increased with ceramming time but the increase was less than in the case of changing temperature.
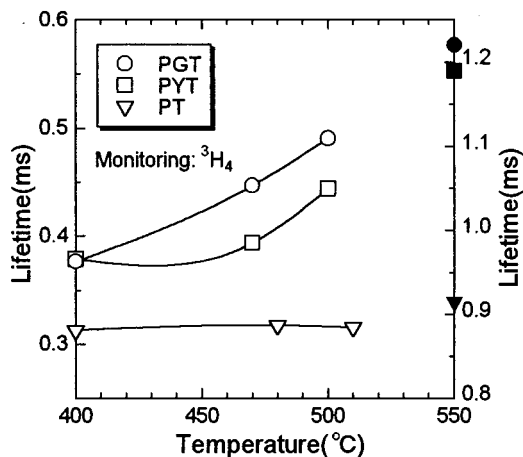
C. Fluorescence properties at lower temperatures

Temperature dependence of fluorescence spectra of the PGT sample cerammed at 470 °C for 4 h is shown in Fig. 5. As a result of XRD measurement, it was revealed that this sample had crystalline phases while keeping good transparency for visible light. With lowering temperature, the structure of the 1.8 μm emission band became sharper. In addition, the 1.4 μm emission band split into two parts under 50 K and the flat range of these peaks became broader than that of 300 K. In addition to these features, several changes of the spectrum structure and emission properties were observed by lowering the temperature. Figure 6 shows the temperature dependence of the integrated intensity of the 1.4 and 1.8 μm emission bands in the PGT sample. While the area of the 1.4 μm band increased slightly, that of the 1.8 μm band decreased slightly with lowering temperature. From this result, we obtained the relative intensity ratio of the 1.4 μm band emission to the 1.8 μm band of the sample with various

FIG. 4. Variation of $^3H_4$ lifetime of Tm^{3+} ion with ceramming temperature. The errors are less than the size of the data symbols. Solid dots represent the data of corresponding crystals.
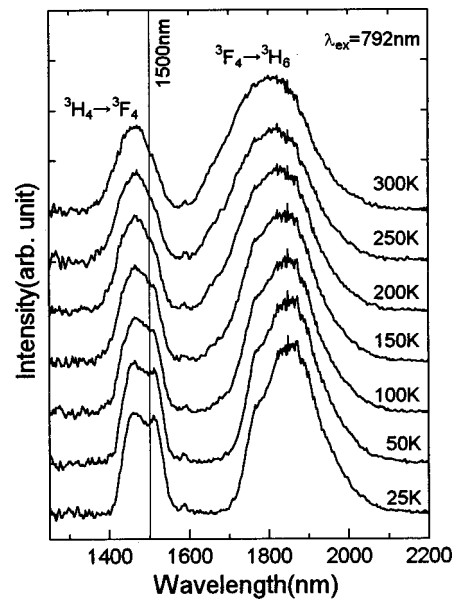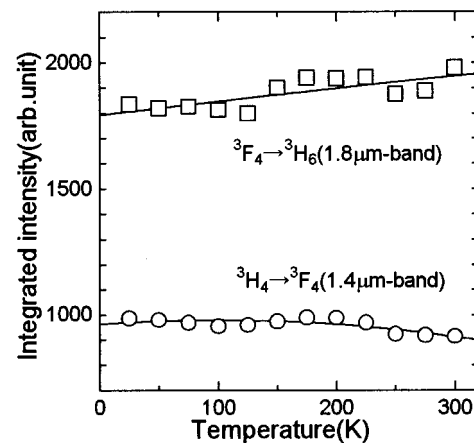

FIG. 6. Temperature dependence of area intensity of the 1.4 and 1.8 μm emission band in transparent glass ceramics containing PbF_2 (PGT sample).
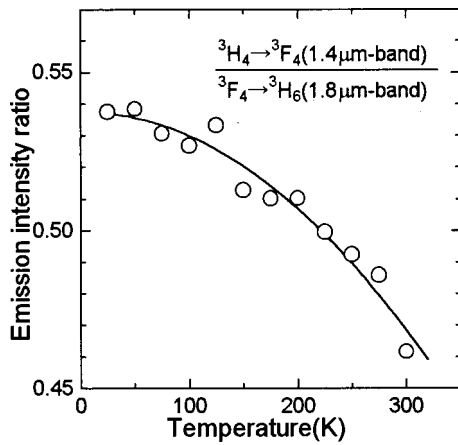
FIG. 7. Temperature dependence of the emission intensity ratio of Tm^{3+}: $^3H_4 \rightarrow ^3F_4$ to $^3F_4 \rightarrow ^3H_6$ in glass ceramics containing PbF_2 (PGT sample).

temperatures, as shown in Fig. 7. With lowering temperature, the relative intensity of the 1.4 μm band emission increased about 15%. Figure 8 shows the temperature dependence of full widths at half maximum of the 1.4 and the 1.8 μm band. While the widths of the 1.4 μm band were almost unchanged, that of the 1.8 μm band decreased as the sample temperature became lower; the width of the 1.8 μm band at 25 K was about 200 cm^{-1} smaller than at 300 K.

IV. DISCUSSION

A. Crystal precipitation and effect of Gd^{3+} or Y^{3+}

From the obtained peak width of the XRD pattern of the PGT and PYT samples, the crystal size of PbF_2 was estimated by the following Sherrer's equation:

$$D = K\lambda / \beta \cos \theta. \qquad (1)$$

The diffraction linewidth β was calculated after subtracting contributions of the strain of crystallites and instrument constant from the measured value.

As heat treatments proceeded, the crystal size in the PGT sample increased and the calculated diameter increased from
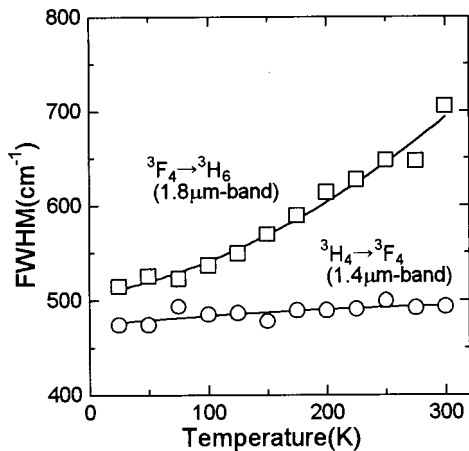

FIG. 8. Temperature dependence of FWHM of the 1.4 and 1.8 μm emission band in transparent glass ceramics containing PbF_2 (PGT sample).

23 nm (470 °C–4 h ceramming) to 44 nm (500 °C–4 h ceramming). The crystal size in the PYT sample was of the same order as PGT. Samples that were heat treated under 470 °C kept good transparency even after cerammization. The main reason for the transparency of these materials is that the crystal size is much smaller than the wavelength of visible light.[9,10]

The fact that no crystalline peaks appeared in the PT sample indicates that the Gd^{3+} or Y^{3+} ion is essential for precipitation of PbF_2, but the reason is not clear. One possibility is to consider the lattice constant of the precipitated crystal. The β-PbF_2 crystal has a cubic structure the lattice constant of which is 0.594 nm. The calculated lattice constant of the PGT sample obtained from the data of d spacing was 0.588 nm (470 °C–4 h ceramming) and 0.590 nm (500 °C–4 h ceramming). Thus it is assumed that the lattice constant of each crystal expanded through heat treatments. The ionic radius of Gd^{3+} is 0.0938 nm, while that of the Pb^{2+} ion is 0.124 nm. Therefore, it is assumed that the Gd^{3+} or Y^{3+} ion-rich phases precipitated as nuclei and then the PbF_2 nanocrystals grew around the nuclei.

B. Change of Tm^{3+} ligand fields

From the change of the fluorescence intensity ratio and the lifetime data, we can see the change of ligand fields of Tm^{3+} ions. The quantum efficiency of fluorescence is expressed by

$$\eta = A/(A + W_p + \tau_{ET}) = \tau_f \times A, \qquad (2)$$

where A is the spontaneous emission probability (radiative transition rate), W_p is the multiphonon decay rate (MPR), τ_{ET} is the relaxation by energy transfer between luminescence centers, and τ_f is the lifetime of the initial level. According to the Miyakawa–Dexter theory, the multiphonon decay rate W_p is expressed by[12]

$$W_p = W_0 \exp(-\alpha \Delta E / \hbar \omega), \qquad (3)$$

where ΔE is the energy gap to the next lower level and $\hbar \omega$ is the phonon energy.

The increase of intensity ratio of the 1460 nm emission to 1800 nm with ceramming times will show that the ligand field of some Tm^{3+} ions changed from oxide environment to fluoride. ΔE of 1.4 μm band (4300 cm^{-1}) is narrower than that of the 1.8 μm band (5500 cm^{-1}) and the former is more sensitive to the change of ligand fields. Therefore, the increase in relative intensity indicates the decrease of host phonon energy with heat treatments. Generally, the cross relaxation of $^3H_4$, $^3H_6 \rightarrow ^3F_4$, $^3F_4$ often occur even though the concentrations of Tm^{3+} ions were sufficiently low;[13] in this case, the contribution of τ_{ET} for the quantum efficiency is not negligible. Therefore, the result also indicates that the influence of the cross relaxation is not significant and contribution of MPR is dominant for the nonradiative loss.

For the PGT sample, the apparent lifetime of the $^3H_4$ level in the glass ceramics was 30% longer than that in the as-made glass and reached almost 500 μs. From Eq. (2), this will also be a result of the change of the ligand field of Tm^{3+} ions through heat treatments and an increase of the quantum
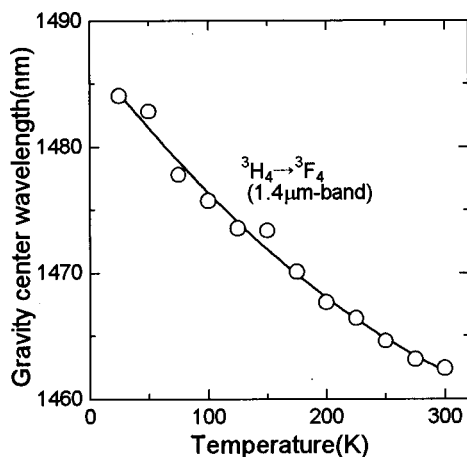
J. Appl. Phys., Vol. 89, No. 2, 15 January 2001

Hayashi, Tanabe, and Hanada   1045

FIG. 9. Temperature dependence of the gravity center of the 1.4 μm emission band in transparent glass ceramics containing PbF$_2$ (PGT sample).

efficiency. However, the lifetime of the reference crystals (1.2 ms) indicate that many Tm^{3+} ions still remained in the glass phase after cerammization.

In the ceramming process, the emission bands became sharper and inhomogeneous widths decreased. This structural change indicates that some of Tm^{3+} ions are incorporated into crystalline sites that have higher symmetry. For lower temperature measurements, almost the same features were also observed. The peak splitting can be due to the Stark effect, which is characteristic of the luminescence center in fluoride crystalline sites.

C. Possibility of S-band amplifier

From spectrum measurement at lower temperature in Fig. 5, we can show the possibility of optical amplifier of the unexplored region. Figure 9 shows the center of gravity of the 1.4 μm band emission with various temperatures of the PGT sample. With lowering temperature, it shifted from 1465 nm at 300 K to 1485 nm at 25 K. At 25 K, the peak wavelength of 1485 nm is longer than the longest edge of S^+-band, so this can be utilized for amplification of the S-band. In addition, as shown in Fig. 5, flat range of this peak was broader at around 50 K than at 300 K. At the same time, the intensity at 1500 nm apparently increased with lowering sample temperature. This was due to the decrease of the multiphonon decay rate. From Fig. 8, it was shown that the decrease of the FWHM of this band was smaller and less than that of the 1.8 μm band. Thus the material can have broader gain range under 50 K for this 1.4 μm band. Furthermore, as shown in Fig. 7, the relative intensity ratio of the 1.4 μm band to the 1.8 μm band of the sample increased

with lowering temperature. All these results support the usefulness of the property of this material. Although a pelche cooling system for coiled fiber may be required, it is considered that making such a condition in the practical device is not as difficult.

V. CONCLUSION

Tm^{3+} ion-doped transparent oxyfluoride glass ceramics containing PbF$_2$ were prepared. It was shown that PbF$_2$ nanocrystals around 20 nm, in size precipitated through the proper heat treatments of the as-made glass. In addition, it was revealed that GdF$_3$ or YF$_3$ was an essential component for crystal precipitation. From the lifetime and fluorescence spectra measurements, we could show that a part of the Tm^{3+} ions was incorporated selectively into the fluoride nanocrystals by ceramization. The emission spectrum of the lower temperature region of the material revealed that it could have a broader and larger gain range under 50 K for the 1.4 μm emission band. Therefore, it is considered that TDF of this material has a potential for the S-band optical amplifier.

[1] J. Kani, K. Hattori, M. Jinno, S. Aisawa, T. Sakamoto, and K. Oguchi, Electron. Lett. **35**, 321 (1999).
[2] S. Tanabe, N. Sugimoto, S. Ito, and T. Hanada, J. Lumin. **87–89**, 670 (2000).
[3] T. Komukai, T. Yamamoto, T. Sugawa, and Y. Miyajima, IEEE J. Quantum Electron. **31**, 1880 (1995).
[4] S. Tanabe, X. Feng, and T. Hanada, Opt. Lett. **25**, 817 (2000).
[5] J. S. Wang, E. Snitzer, E. M. Vogl, and G. G. Sigel, J. Lumin. **60–61**, 145 (1994).
[6] T. Kasamatsu, Y. Yano, and H. Sekita, Proceedings OAA'1999, Post Deadline Paper 1.
[7] S. Aozasa, T. Sakamoto, T. Kanamori, K. Hoshino, and M. Shimizu, Electron. Lett. **36**, 418 (2000).
[8] S. Tanabe, K. Tamai, K. Hirao, and N. Soga, Phys. Rev. B **47**, 2507 (1993).
[9] Y. Wang and J. Ohwaki, Appl. Phys. Lett. **63**, 3268 (1993).
[10] P. A. Tick, N. F. Borrelli, L. K. Cornelius, and M. A. Newhouse, J. Appl. Phys. **78**, 6367 (1995).
[11] P. A. Tick, N. F. Borrelli, and I. M. Reaney, Opt. Mater. **15**, 81 (2000).
[12] T. Miyakawa and D. L. Dexter, Phys. Rev. B **1**, 2961 (1970).
[13] A. Brenier, C. Pedrini, B. Moine, J. L. Adam, and C. Pledel, Phys. Rev. B **41**, 5364 (1990).